

Exploring frontier areas using 2D seismic and 3D CSEM data, as exemplified by multi-client data over the Skrugard and Havis discoveries in the Barents Sea

Pål T. Gabrielsen,^{1*} Peter Abrahamson,² Martin Panzner,¹ Stein Fanavoll¹ and Svein Ellingsrud¹

Abstract

There is new and growing enthusiasm for hydrocarbon exploration in the Barents Sea after three recent discoveries: Skrugard, Havis, and Norvarg. We demonstrate how using wide-azimuth 3D controlled-source electromagnetic (CSEM) and 2D seismic data together can improve the identification of prospective areas in the region. An interpretation workflow is presented to show how the challenging resistivity background in the Barents Sea is handled. To do this, we introduce a new inversion attribute called the anomalous vertical resistivity. The inversion attribute is co-visualized with 2D seismic data and used to estimate recoverable reserves. The workflow is illustrated on both synthetic and real data for the Skrugard and Havis discoveries. Both discoveries are identified on CSEM maps and by integrating CSEM data with seismic data. In addition, a new lead is identified. We show that CSEM data carries structural information and that the horizontal resistivity trends can be used with 2D seismic data and well logs to interpret the distribution of good-quality sands. Hydrocarbon reserve calculations based on the 3D CSEM data for the Skrugard and Havis discoveries have P50 values consistent with the publicly available reserve estimates. The reserve estimate for the new lead also shows significant potential.

Introduction

There is new and growing enthusiasm for hydrocarbon exploration in the Barents Sea after three recent discoveries: Skrugard and Havis, both having substantial proven oil reserves, and the gas discovery, Norvarg. This enthusiasm is further encouraged by the Norwegian government, which has announced 72 new blocks in the Barents Sea for the 22nd licensing round. Most of the announced blocks are in the Bjørnøya and Fingerdjupet basins, leaving large parts of the Barents Sea still virtually unexplored and open.

More than 90 exploration wells have been drilled so far on the Norwegian side of the Barents Sea, mainly during the 1980s and the last decade. Most of those wells are classified as being dry or with shows only. However, the wells verify the existence of a large petroleum system in the area. After 30 years of exploration, only one field is in production (Snøhvit) and one other is being developed (Goliat) in the Norwegian part of the Barents Sea. The three recent discoveries are therefore revitalizing interest in the Barents Sea as a hydrocarbon province and putting a totally new focus on the whole region.

EMGS and MultiClient Geophysical (MCG) have acquired extensive multi-client wide-azimuth 3D CSEM

and 2D seismic data across the Barents Sea (Figure 1). The multi-client CSEM data were acquired using a rolling 3 km × 3 km receiver grid with the aim of achieving an effective scan of the area. The EM source is run above all the N–S oriented receiver lines while two neighbouring receiver lines on each side of the towing stay on the seabed. This ensures an acquisition geometry gathering both inline and broadside data. The 2D seismic data cover the Bjørnøya Basin and Fingerdjupet Sub-basin with a dense 2D grid and include tie lines through most of the well locations in the Barents Sea.

In this paper, we show how the combination of 2D seismic and 3D CSEM data can be used as an important decision-making tool for initial interpretation, risking, and reserves estimation in frontier areas. We illustrate this by using data covering both the Skrugard and Havis discoveries on the Polheim Sub-platform (Figure 1). The area is ideal for demonstrating our objectives, as the discoveries can be used as calibration points. Multi-client seismic and CSEM data, public data from Well 7219/9-1, and seismic horizons interpreted from 2D seismic data are used in this study. Note that the discoveries made under the licence are not based on the work presented here.

¹ EMGS, Stiklestad v1, 7040 Trondheim, Norway.

² MultiClient Geophysical, Stasjonsveien 18, 1396 Billingstad, Norway.

* Corresponding author, E-mail: ptg@emgs.com

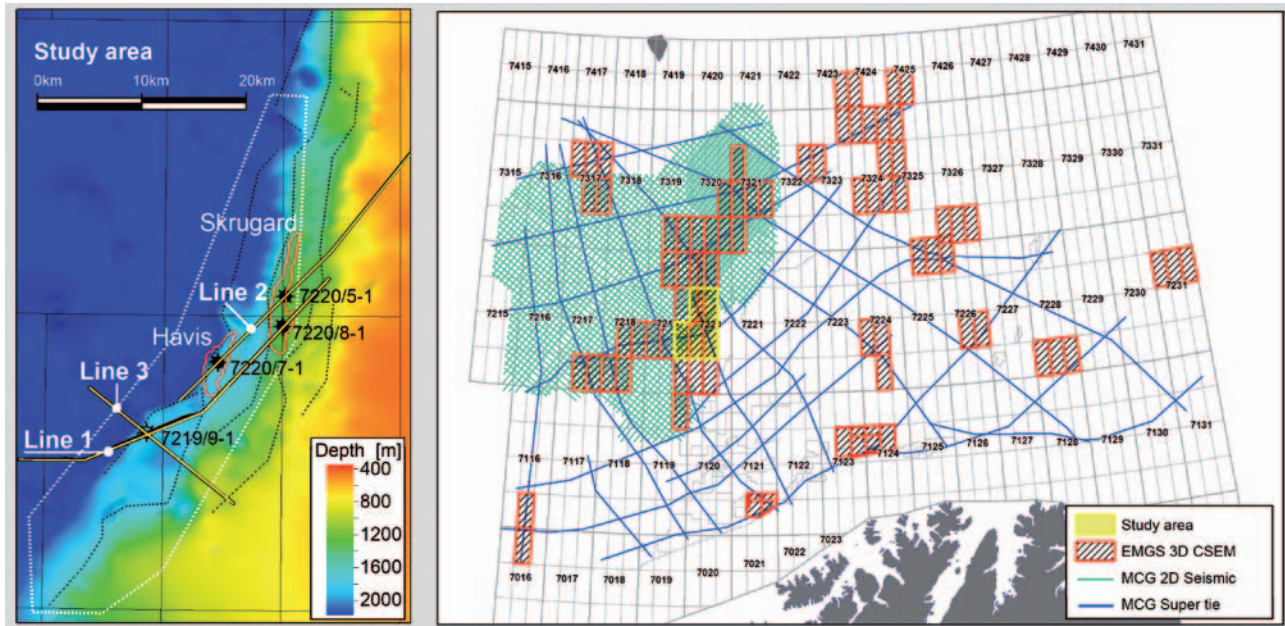


Figure 1 Left: overview map of the study area, outlined by the white dashed line, showing the Base Cretaceous depth map interpreted from 2D seismic data, an interpretation of the major faults (black dotted lines), the locations of drilled wells, the published prospects (outlined in red), and the 2D lines presented in this paper (yellow). Right: Regional map showing the study area and coverage of multi-client 2D seismic data from MCG and of multi-client 3D CSEM data from EMGS in the Barents Sea.

From a CSEM perspective, the Barents Sea offers both simple and complex settings (Fanavoll et al., 2012; Gabrielsen et al., 2012). Stratigraphic traps in the Tertiary are an ideal setting for the methodology with their fairly uniform background geology and shallow target burial depths. A more challenging interpretation setting is introduced by the strong anisotropy factor often associated with layers in the Cretaceous and the Triassic. For example, we have observed from CSEM data that the Triassic can have an anisotropy factor ranging from five to 10 and high vertical resistivities between 50 and 150 Ω m in its brine-saturated state. Structurally complex areas such as the Bjørnøyrenna fault complex can cause strong lateral changes in the background resistivity, which are probably due to thickness variations and the burial depth of the Cretaceous. Such resistivity variations need to be accounted for when interpreting the inverted CSEM results.

To handle variation in the background resistivity, Hesthammer et al. (2010) introduced the normalized anomalous response (NAR) for the interpretation of CSEM data attributes. This attribute is the normalized magnitude response after subtracting an interpreted background trend. Using their database of 84 wells, of which 50 wells are commercial discoveries, they showed that a NAR value larger than 15% correctly predicted a discovery success in 40 out of the 50 wells. A key factor in this prediction is interpreting the background trend. We suggest that the horizontal resistivity model could be a key to understanding the background resistivity because horizontal resistivity, R_h , is a common parameter for independent measurements, by CSEM and magnetotelluric surveys and resistivity logs, and the R_h model from CSEM

data is insensitive to thin horizontal resistors. The difference in sensitivity between the vertical resistivity, R_v , and the horizontal resistivity is also used by Alcocer et al. (2012) in the Gulf of Mexico, where thin resistors (potential reservoirs) are interpreted with increased confidence where the electrical anisotropy factor, R_v/R_h , is anomalously high.

Interpreting prospective areas based on CSEM data alone is very challenging, and in frontier areas usually only 2D seismic data available. However, the combination of the two different data types can be a powerful tool in exploration. 2D seismic data can help in the interpretation of resistive trends and anomalies in CSEM data for better understanding of the nature of resistivity variations in the subsurface. At the same time, the lack of 3D information in 2D seismic data can be compensated for by the 3D resistivity information obtained from CSEM data. CSEM data carries important structural and geometric information that can potentially help the interpretation of 2D seismic data. Once a prospective area has been identified, 3D CSEM data can be used to estimate the net rock volume probability distribution which, in turn, provides information of hydrocarbon reserves.

In this paper, we have applied an unconstrained anisotropic 3D inversion (Morten and Bjørke, 2010) on the wide-azimuth CSEM data to obtain a 3D resistivity volume of the subsurface. The start model used for the inversion is built by using seismic horizons picked on 2D seismic data with a constant resistivity for each layer. Based on the CSEM inversion results and the 2D seismic data, we demonstrate three interpretation methodologies illustrated both by synthetic and real data examples. First, we show how a complex resistivity background can mask reservoirs

and how this problem can be tackled by using the sensitivity difference in the R_v and R_h models. To do this, we introduce a new inversion attribute called anomalous vertical resistivity, AR_v . Second, we show how co-visualization can improve the interpretation of both seismic and CSEM data. Finally, we estimate hydrocarbon reserves at an early exploration stage using only 3D CSEM data.

Handling the background resistivity variation

To combine information from 2D seismic and 3D CSEM data properly, we first need to consider the CSEM interpretation challenge caused by strong variations in background resistivity. There can be wide variations in the electrical background resistivity in the structurally complex study area. Figure 2a shows a map of the inverted vertical resistivity in the area, which reveals a strong regional variation overlain by two resistive anomalies. The observed lateral resistivity variations are interpreted as being mainly associated with the complex Bjørnøyrenna fault system, as the resistivity variations follow the overlain fault boundaries. The change in geology is seen from the seismic section in Figure 2b.

The resistivity map shows that the Havis discovery is associated with a resistive anomaly whereas the Skrugard discovery is not evident at this stage. We will later show that this is caused by the background resistivity variation, and that it is essential that the regional trend is removed for CSEM anomaly interpretation. We do that by taking advantage of the different sensitivity the CSEM data exhibits to the horizontal and vertical resistivities in the subsurface.

When performing anisotropic unconstrained 3D inversion of CSEM data, we recover both horizontal and vertical resistivity in the subsurface, providing two separate earth models. The sensitivities to the vertical and horizontal resistivity depend to a large extent on the acquisition geometry. A wide-azimuth 3D CSEM acquisition, such as

used in the Barents Sea, provides both inline and broadsided data. The inline configuration is dominated by the TM mode and is very sensitive to the vertical resistivity, whereas the broadside configuration is dominated by the TE mode, which is sensitive to the horizontal resistivity in the subsurface (Lu and Xia, 2007). This is similar to magnetotelluric measurements, which are only sensitive to the horizontal resistivity. However, only the TM mode is sensitive to thin resistive layers (Eidesmo et al., 2002; Løseth, 2007), so only the vertical resistivity model will image thin resistors. The horizontal resistivity model will not image thin resistive layers; rather it will model large-scale structures, conductors, and background resistivity trends.

We illustrate the difference in sensitivity by using a synthetic example representing the Skrugard discovery. The earth model (Figure 3a) was constructed using regional depth-converted seismic horizons with a varying background resistivity in each layer. A target was inserted in the Jurassic, using the Skrugard outline from the Norwegian Petroleum Directorate, with a varying thickness and a constant resistivity of 40 Ω m. Synthetic CSEM data were generated by running 3D forward modelling with a receiver spacing and towline configuration similar to the multi-client surveys acquired by EMGS in the Barents Sea. The synthetic data were then used as input to an unconstrained 3D inversion.

Figure 3b shows the unconstrained inversion results for the synthetic CSEM data. The results clearly show that only the vertical resistivity model images the resistive target; the horizontal resistivity model does not show any resistivity increase at the target location. The latter model only images the background resistivity. Figure 3c shows the inverted results in map view. The maps show the average resistivity in the target interval between the black solid lines marked in the cross-sections (Figure 3b). Vertical resistivity images the target, but is also overlain by the regional trend:

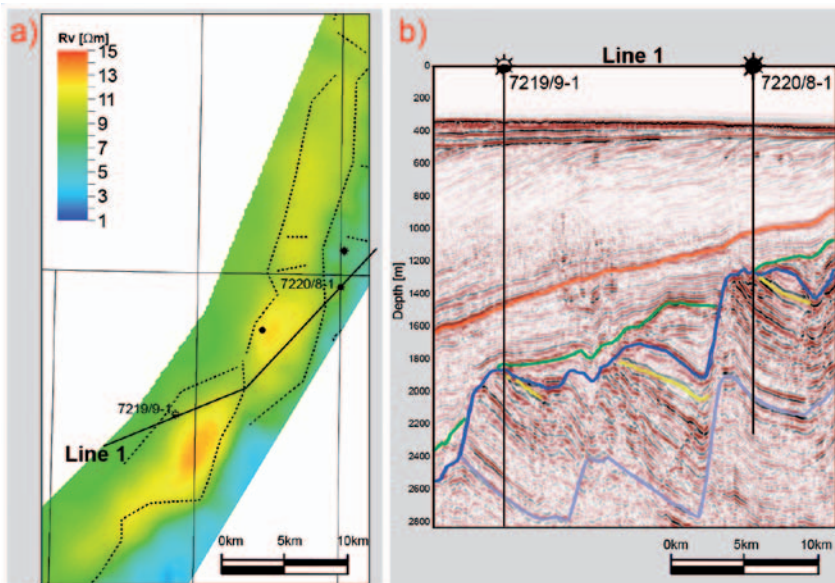


Figure 2 (a) Average R_v map from unconstrained 3D CSEM inversion, calculated using a 1000-m thick window centred around the Base Cretaceous unconformity. (b) Interpreted seismic section: orange—base Tertiary; green—top Lower Cretaceous; blue—base Cretaceous; yellow—Middle-Lower Jurassic; purple—top Snadd Formation.

$$R_v^{CSEM} \approx R_v^{Background} + R_v^{Thin\ resistor} \quad (1) \quad AR_v = R_v^{CSEM} - R_v^{Background} = R_v^{Thin\ resistor} \quad (5)$$

The vertical resistivity map (Figure 3c) shows that it would be difficult to separate the target anomaly (inside the black polygon) from the overall regional trend (increasing to the NNW). On the other hand, the horizontal resistivity map (Figure 3c) only shows the background resistivity variations without the target.

$$R_h^{CSEM} \approx R_h^{Background} \quad (2)$$

We have calculated a map of the anisotropy factor (Figure 3c), which is the R_v model divided by the R_h model:

$$ANI^{CSEM} = \frac{R_v^{CSEM}}{R_h^{CSEM}} \approx \frac{R_v^{Background} + R_v^{Thin\ resistor}}{R_h^{Background}} \approx ANI^{Background} + ANI^{Thin\ resistor} \quad (3)$$

This map is interesting because it nicely isolates the target with anomalously high apparent anisotropy values from the gently varying regional anisotropy outside the target. The true regional anisotropy outside the target is well recovered by the unconstrained inversion, whereas the anomalous anisotropy within the target is reconstructed too high (the true target anisotropy is 1). This illustrates that it is possible to estimate the trend of vertical background resistivity, $R_v^{Background}$, in the target area from the R_b model and an average background anisotropy factor, $ANI^{Background}$.

$$R_v^{Background} \approx R_h^{CSEM} ANI^{Background} \quad (4)$$

Obtaining the vertical background resistivity, as described in Equation 4, enables us to solve the challenge of a varying background resistivity and isolate thin resistors that can be associated with hydrocarbon targets. For this, we introduce a new inversion attribute called anomalous vertical resistivity, AR_v :

In addition to identifying thin resistors (potential prospective areas) the attribute AR_v can be used directly to estimate the net rock volume of the anomalous resistive body. Hence, if the anomalous resistive anomaly is caused by a hydrocarbon charged reservoir, this volume is directly linked to hydrocarbon volume in place. Baltar and Roth (2012) describe how an average vertical resistivity map can be used as input to a Monte Carlo simulation predicting the net rock volume of the hydrocarbon charged reservoir. In our case such a map will also be strongly influenced by a laterally varying background resistivity and can therefore not be used for net rock volume calculation. Instead, it will be more appropriate to use the AR_v attribute for these calculations.

Interpretation workflow

Our interpretation workflow is designed to handle strong background resistivity trends. Figure 4 summarizes the workflow by using the data from the synthetic example discussed above. The $R_v^{Background}$ and AR_v maps are constructed using Equations 4 and 5. The blue in the AR_v map represents values close to zero and means no anomaly, i.e., the vertical resistivity reconstructed by the unconstrained inversion follows the expected background trend.

In this map, the Skrugard anomaly is very well defined in comparison to the original R_v map. The AR_v cube generated can be integrated with seismic data in order to interpret the origin of the resistive anomaly. If it is likely that the anomaly is caused by hydrocarbons, the AR_v map can be used as input for hydrocarbon reserve estimates. It is important that such an estimate is first carried out on a synthetic data example before it is applied to real data. This is because the reconstruction of the target volume can be underestimated due to decreasing

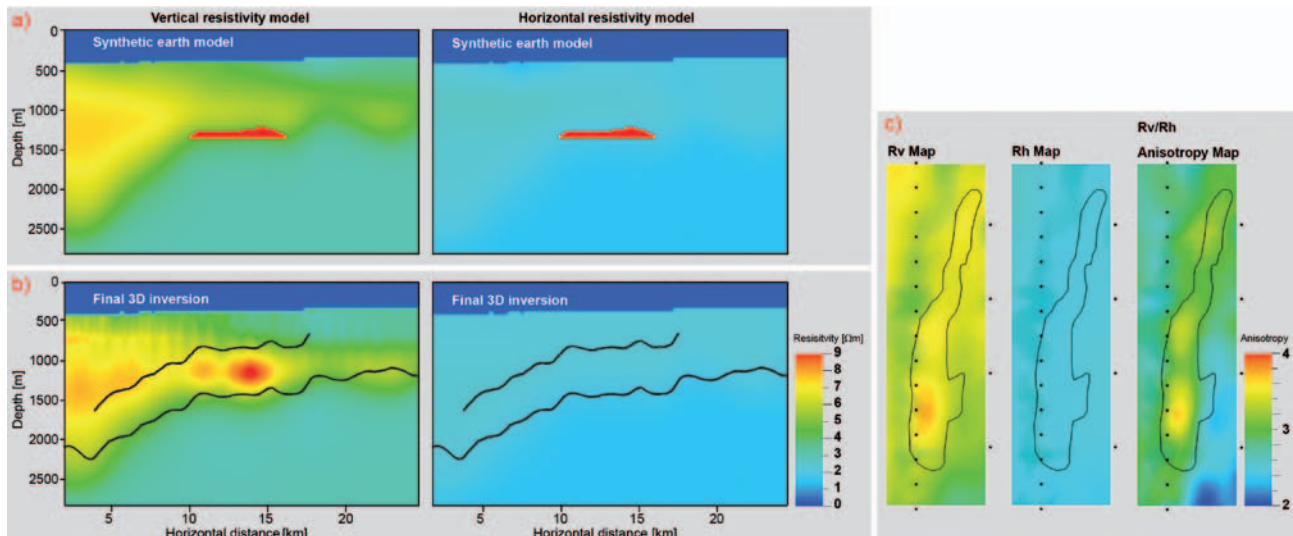


Figure 3 Unconstrained 3D inversion of synthetic data. (a) Resistivity earth model representing the Skrugard discovery with the R_v model on the left and the R_h model on the right. (b) Only the inverted R_v model images the thin resistive target. The solid lines show the 600-m window used to calculate (c) the average resistivity maps for R_v and R_h , and the anisotropy factor, ANI. Black squares are the receiver positions.

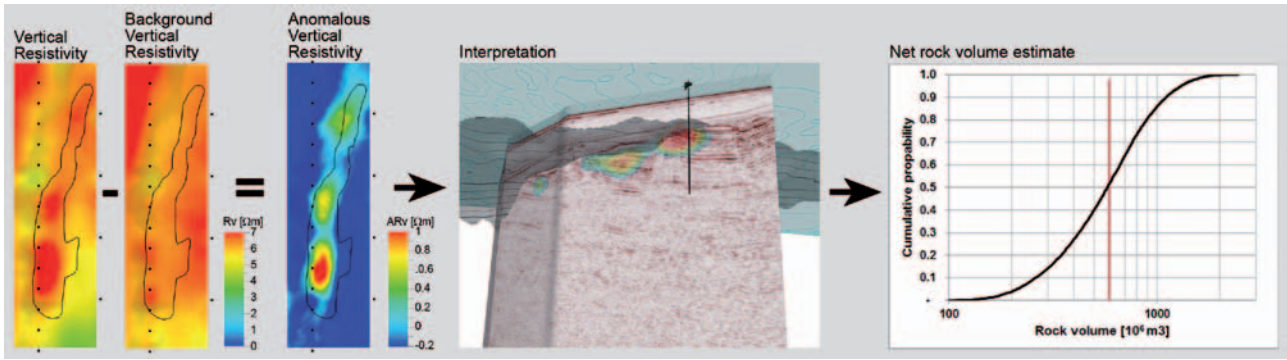


Figure 4 Synthetic example of Skrugard demonstrating the interpretation workflow.

sensitivity with depth and coarse receiver sampling. In our synthetic example, it was necessary to apply a correction factor of 1.28 in order to obtain a correct volume estimate (red vertical line). This correction factor is found by taking the relationship between the true reservoir volume in the synthetic model and the calculated volume using the synthetic anomalous vertical resistivity map together with the reservoir resistivity used in the synthetic model. We use this correction factor later in this study when we estimate reserve volumes on real data. The main cause of this underestimation is most likely the sparse receiver sampling (3 km × 3 km) used for the multi-client data. A more dense acquisition pattern would give a more accurate volume estimate.

Interpretation of the real data

Well 7219/9-1 was drilled in 1988 at the crest of a fault block with the main targets in the Jurassic sandstones (the Stø, Nordmela and Tubåen formations). A total thickness of 350 m of sand was encountered for the three formations, with porosities in the range 16–18%. In addition, a thinner section of sand in the Lower Cretaceous is found (the Knurr Formation). The well was dry with oil shows. The resistivity log from the well is given in Figure 5. Note the low horizontal resistivity recordings (<1 Ωm) in the Jurassic sand interval, especially for the Stø Formation.

An average R_h map from inverted 3D CSEM data is given in Figure 6a. The map is calculated with a 1000 m thick window centred on the Base Cretaceous unconformity. According to the synthetic study and Equation 2, this map provides the regional resistivity trends in the area. There are areas with very low resistivity (light to dark blue) to the east and south, where the Jurassic is shallower than in the west. From the low resistivity reading of the water-filled sands in Well 7219/9-1 (Figure 5), we suggest that these low resistivity areas could indicate areas with porous sands of significant thickness. Figure 7 illustrates how this interpretation could map the distribution of good-quality sand in the area if only 3D CSEM data, one calibration well, and 2D seismic data were available. As explained previously, the R_h model is not sensitive to hydrocarbon intervals within a thick sand package, since it is not sensitive to thin resistors.

Figure 6b shows the average R_v map calculated for the same 1000 m thick window as the R_h model. It is important to stress that large windows should be used for these maps, as they will be used later for reserve estimates. For this calculation, it is essential that the entire anomaly is included. As previously discussed, the R_v map provides information about thin horizontal resistors in addition to the background resistivity trends (Equation 1). Two main resistivity anomalies can be identified in this map. One is at the location of the Havis discovery and the other is southeast of Well 7219/9-1. We name the latter anomaly Lead 1. As described earlier, no significant anomaly is associated with the Skrugard discovery.

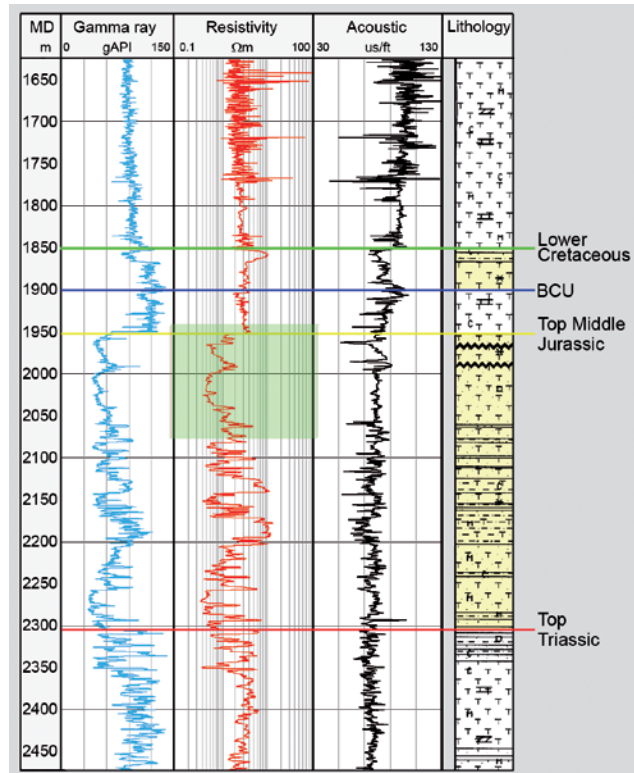


Figure 5 Resistivity log from Well 7219/9-1, which was drilled in 1988. Low resistivity values are found for the Jurassic sands, especially in the Stø Formation (highlighted in pale green). Yellow shading in the lithology column indicates the interval with cored sand (source npd.no).

Figure 6c shows the AR_v , as defined in Equation 5. The $R_{v\text{Background}}$ is constructed according to Equation 4 by multiplying the R_h model (Figure 6a) by a regional anisotropy factor of 3.9. This value is found by inspecting the histogram of the calculated anisotropy within the given depth window. On this map, three anomalies are seen where Havis and Lead 1 are already identified in the R_v map. In addition, the Skrugard

discovery is now identified, which suggests that $R_{v\text{Background}}$ has been successfully removed to leave only anomalous resistivity bodies. Note also that the previously identified area in the south associated with a low R_h (possible sand), like the Skrugard area, does not have an anomalous vertical resistivity. This is an important calibration point for ruling out that the anomalous resistivity is purely a function of areas with low horizontal

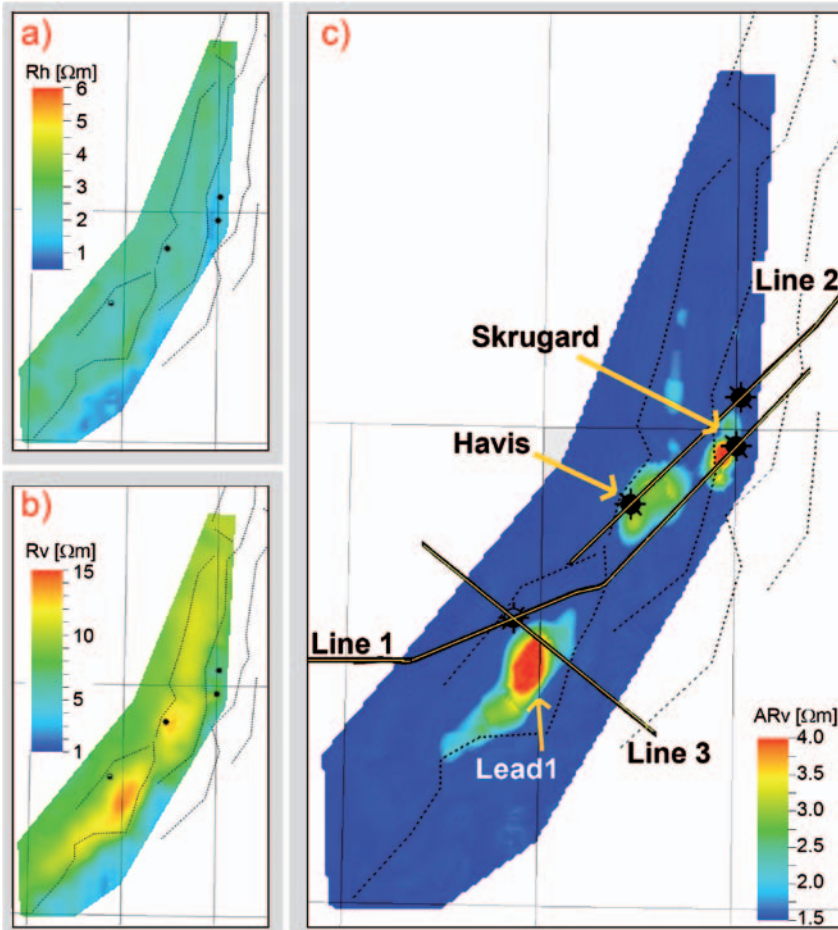


Figure 6 Average CSEM maps from final unconstrained 3D inversion results calculated in a window from 500 m above to 500 m below the Base Cretaceous unconformity horizon shown in Figure 1: (a) horizontal resistivity, R_h ; (b) vertical resistivity, R_v ; (c) anomalous vertical resistivity, AR_v .

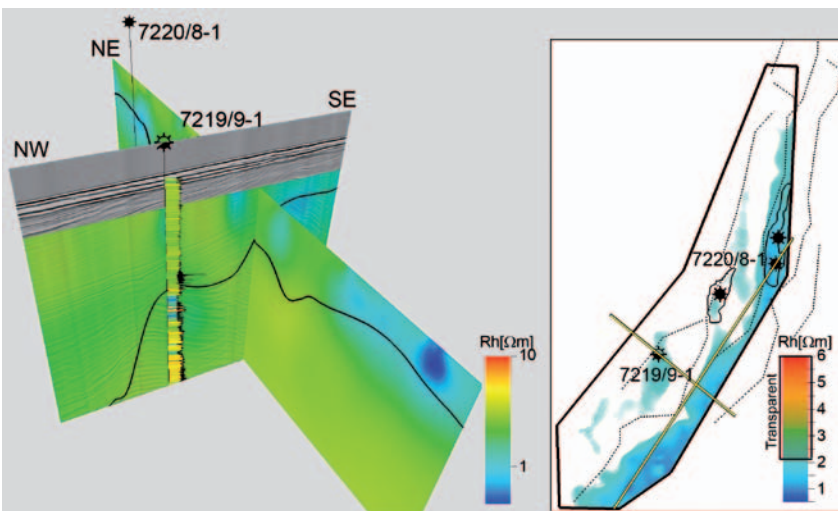


Figure 7 Horizontal resistivity displayed with seismic data. Low resistivity zones (blue and light blue) may indicate good-quality sands. The map is the same as Figure 6a except that the colour scale is made transparent above $2.1 \Omega\text{m}$.

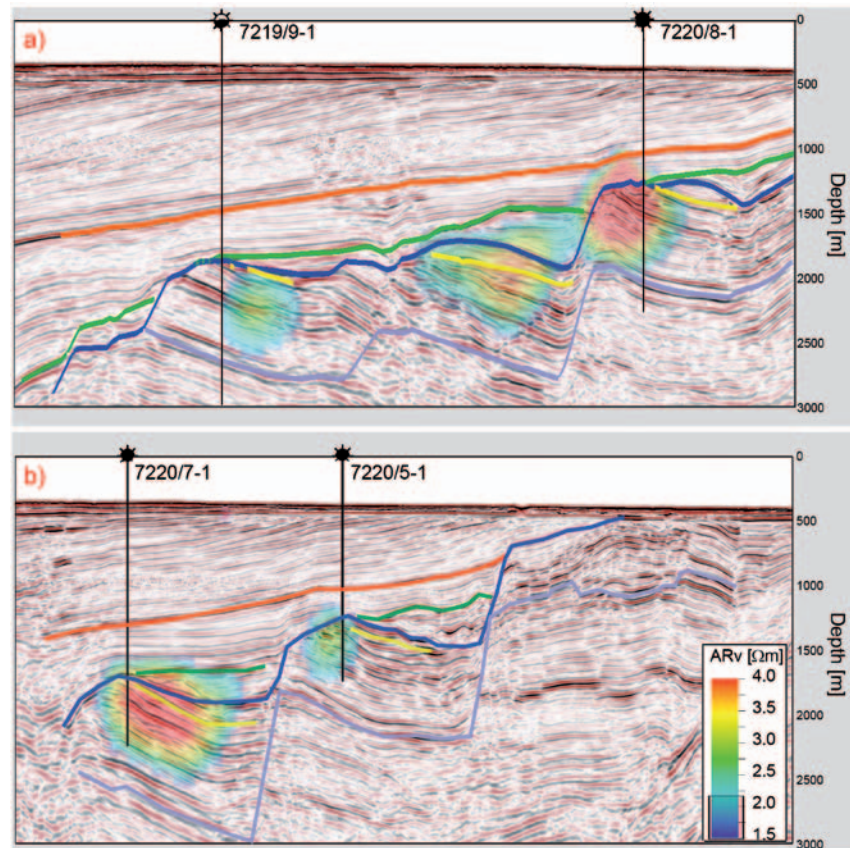


Figure 8 2D seismic lines from MCG programme 2010 and 2012: (a) Skrugard discovery well, the edge of the Havis discovery, and the dry well (line 1 in Figure 1); and (b) the Skrugard appraisal well and the Havis discovery well (line 2 in Figure 1). Overlain is the AR_v from the CSEM data along with the interpreted horizons and well locations. Colour scale is made transparent below 2.2 Ωm .

resistivity. The results suggest that this particular area is not hydrocarbon-charged or that the net rock volume associated with the structure is too small to be detected by using CSEM. Also, note that the resistive anomaly named Lead 1 terminates just to the east of the position of Well 7219/9-1.

Skrugard and Havis discoveries

The Skrugard and Havis discoveries are found in faulted blocks in the Early–Middle Jurassic. A 2D seismic tie-line between wells 7219/9-1 (shows) and 7220/8-1 (the Skrugard discovery) is given in Figure 8a. Overlying the seismic data is the AR_v attribute and an interpretation of some key horizons. A resistive anomaly is placed at the crest of the fault block where the Skrugard discovery is located. No anomaly is associated at the position of the dry well in the west. On this particular seismic line, the Havis discovery is located in the fault block in the middle of the section, but the line intersects just south of the interpreted Havis outline published. The Havis discovery is clearly seen as an anomaly on a different seismic line through the discovery well, 7220/7-1 (Figure 8b). This particular line also goes through the Skrugard appraisal well, 7220/5-1, where a weaker anomaly is seen at the Skrugard location.

Lead 1

The anomaly denoted as Lead 1 is different from the Skrugard and Havis anomalies in that it is not located at the crest of a fault block, but in a more down-dip position (Figure 9).

In addition, it is adjacent to Well 7219/9-1, which is reported as dry with shows in the main target reservoir. Therefore, different models must be suggested in order to explain this anomaly:

- a) On one of the lines (Figure 8a), a flat event east of Well 7219/9-1 can be seen in the Stø Formation, which points to the possibility of a fluid contact and suggests a deeper reservoir compartment. However, this requires that the minor fault is sealed up-dip, which is rather unlikely, as shows were reported in the well in the same reservoir. In addition, the flat event is not observed on other lines crossing the same fault block.
- b) If a charged compartment in the Stø Formation is not the source of the anomaly, it is likely to be sourced from a shallower stratigraphic level in the syn-rift section of the Upper Jurassic and Lower Cretaceous. This could be either hydrocarbon-charged syn-rift sands (the Knurr Formation) or a significant local increase in both the thickness and the resistivity of the Upper Jurassic source rock (Hekkingen Formation), which is known to be of fairly high resistivity (e.g., Well 7219/8-1).

It is difficult to determine which model is the more probable. Therefore, the interpretation uncertainties should be quantified through a risking process. When combined with volume estimation described below, it will provide valuable input for deciding whether to drill or not.

Reserve volume estimates

We can use the AR_v obtained from the interpretation workflow as input for estimating the net rock volume for each of the identified anomalies. Assuming the anomalous resistivity is caused by hydrocarbons, the calculated net rock volume can be converted to reserve volumes using the following formula:

$$N = \frac{V_b \phi (1 - S_w) R}{B_{oil}} \quad (6)$$

where N = recoverable reserves; V_b = bulk net rock volume, estimated from CSEM data; ϕ = porosity; S_w = water saturation; R = recovery factor; and B_{oil} = formation volume factor for oil.

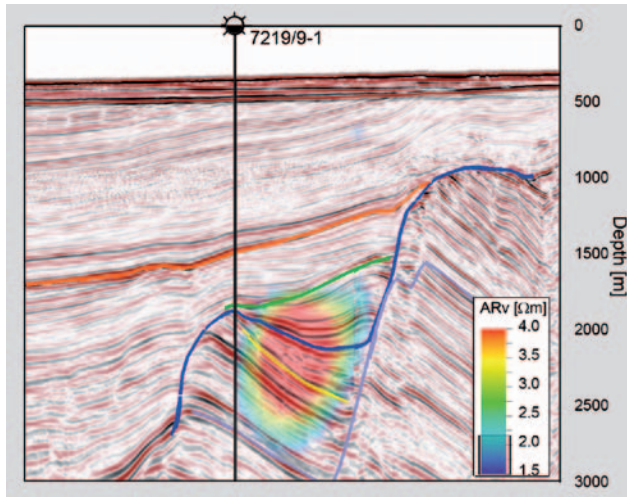


Figure 9 2D seismic line from MCG programme 2009 (line 3 in Figure 1) showing Lead 1 positioned down dip of the dry well. Overlain is the AR_v from the CSEM data along with the interpreted horizons and well locations. Colour scale is made transparent below 2.2 Ωm .

The input to the volume calculation is the AR_v map in Figure 6c. We assume a uniform distribution for the target resistivity of $40 \pm 30 \Omega m$. In addition, we scale the rock volumes using a Gaussian distribution with median value of 1.28 and a standard deviation of 0.2. This scaling factor is introduced in the interpretation workflow section to compensate for the volume underestimation quantified by the synthetic inversion study. To convert the estimated net rock volume to reserve estimates, we use Equation 6. For simplicity, we apply constant values for the other parameters (Table 1). It is important to note that the authors do not have access to any real data about these parameters, so their results may vary from what is used for the publicly available reserve estimates.

The reserves estimates based on the CSEM data and the parameters in Table 1 are shown in Figure 10. As constant values are used in the simulation of Equation 6, except for the bulk net rock volume, the variance is due to the CSEM uncertainties: mainly the uncertainty in the target resistivity, but also to some extent the uncertainties in estimating the background resistivity in Equation 4. The P50 estimates for Havis and Skrugard are well within the reserve volume

Parameter	Value
Porosity, ϕ	18%
Water saturation, S_w	30%
Recovery factor, R	40%
Formation volume factor, B_{oil}	1.2
Net rock volume, V_b	AR_v map

Table 1 Parameter values used to calculate recoverable reserves.

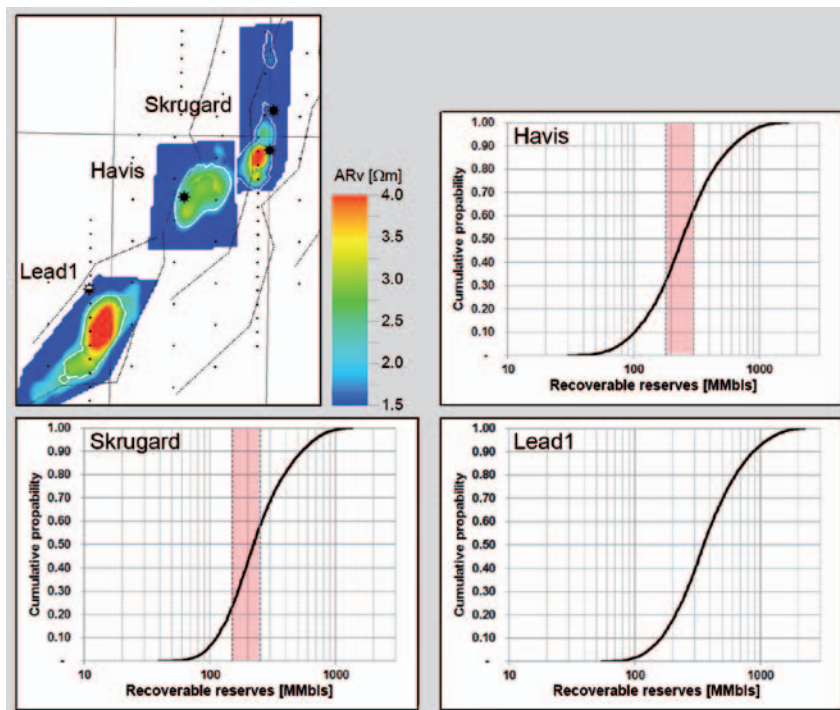


Figure 10 Reserve volume estimates. The P50 values of recoverable reserves based on the CSEM data presented here are within the estimates for Skrugard and Havis published by the licensee (shaded area). Note that the volume estimate for Lead 1 is significant.

ranges published by the licensee (vertical grey dotted lines). These are 180–300 MMbbl and 150–250 MMbbl, respectively. Also, note that the volume estimate for Lead 1 has a P50 of 350 MMbbl, which should make this lead interesting for further detailed exploration in order to understand which geological model is the more likely cause of this anomaly.

Conclusion

Large parts of the Barents Sea are regarded as frontier areas: from the southwestern area, including the Bjørnøya and Fingerdjuvet basins, across the Hoop High and the Bjarmeland Platform and up to the completely unexplored Grey Zone, which has now been divided into a Norwegian and a Russian part. Using multi-client data acquired over the Skrugard and Havis discoveries in the Barents Sea, we have demonstrated that the combination of 2D seismic and 3D wide-azimuth CSEM data can be a powerful tool in the early exploration phases, including the identification of prospects, risk ranking, and the estimation of recoverable reserves.

Both discoveries are identified from 3D CSEM data, and reserve volumes have been calculated with P50 values well within the public volume estimates given by the licensee. In addition, the CSEM data identify a new lead. Co-visualization with a seismic 2D line suggests two possible geomodels that can explain this lead: a false positive anomaly created by local thickening of the source rock, or a true positive CSEM anomaly in the syn-rift sediments. Furthermore, areas with low resistivity are observed in the inverted R_h maps. These results along with the 2D seismic data and the resistivity log of Well 7219/9-1 can be used to interpret the distribution of good reservoir-quality Jurassic sands.

Through both synthetic and real data examples, we have shown that we can handle challenges of complex background resistivities and highlight thin resistors (hydrocarbon reservoirs) by combining regional anisotropy and horizontal resistivity information. This is because the inverted horizontal resistivity model is mainly sensitive to the background resistivity and not to thin resistors. However, the vertical resistivity model is sensitive to both. We have suggested a workflow where a background vertical resistivity model is created by multiplying the horizontal resistivity model by the regional anisotropy factor. This background is subtracted from the CSEM inverted vertical resistivity to obtain anomalous vertical resistivity, AR_v . This attribute will highlight potential prospective areas.

3D CSEM data is shown to be a powerful tool for reserve estimation. When a prospect has been identified by combining CSEM data with seismic data, the net rock volume associated with the CSEM anomaly can be calculated because CSEM data is sensitive to the volume of anomalous resistive rock. In our

example, we ran a Monte Carlo simulation to establish the net rock volume distribution and hence the reserves distribution. The P50 values for the Skrugard and Havis discoveries are within the limits provided to the public. The synthetic and real data examples demonstrate that reliable reserve estimates can be obtained at a very early exploration stage by using 3D CSEM data.

We have shown that the combination of 2D seismic and 3D CSEM data improves the ability to risk prospects and estimate reserve volumes at an early exploration stage. This improves decision making in selecting areas of interest for further exploration, denser acquisition of seismic and EM data, and optimal drilling location.

Acknowledgements

We thank Stig Arne Karlsen for help with the illustrations used in this paper.

References

- Alcocer, J.A.E., García, M.V., Soto, H.S., Roth, F., Baltar, D., Gabrielsen, P. and Paramo, V.R. [2012] Experience from using 3D CSEM in the Mexican deepwater exploration program. *82nd SEG Annual International Meeting*, Expanded Abstracts, 5.
- Baltar, D. and Roth, F. [2012] Reserves estimation from 3D CSEM inversion for prospect risk analysis. *74th EAGE Conference & Exhibition*, Extended Abstracts, E028.
- Eidesmo, T., Ellingsrud, S., MacGregor, L., Constable, S., Sinha, M., Johansen, S., Kong, F. and Westerdahl, H. [2002] Sea bed logging (SBL), a new method for remote and direct identification of hydrocarbon filled layers in deepwater areas. *First Break*, 20(3), 144–152.
- Fanavoll, S., Ellingsrud, S., Gabrielsen, P., Tharimela, R. and Ridyard, D. [2012] Exploration with the use of EM data in the Barents Sea: the potential and the challenges. *First Break*, 30(4), 89–93.
- Gabrielsen, P., Shantsev, D.V. and Fanavoll, S. [2012] 3D CSEM for hydrocarbon exploration in the Barents Sea. *5th Saint Petersburg International Conference & Exhibition, EAGE*, Extended Abstracts, C002.
- Hesthammer, J., Fanavoll, S., Stefatos, A., Danielsen, J.E. and Boulaenko, M. [2010] CSEM performance in the light of well results. *The Leading Edge*, 29, 34–41.
- Lu, X. and Xia, C. [2007] Understanding anisotropy in marine CSEM data. *77th SEG Annual International Meeting*, Expanded Abstracts, 633–637.
- Løseth, L.O. [2007] *Modelling of Controlled Source Electromagnetic Data*. PhD thesis, Norwegian University of Science and Technology.
- Morten, J.P. and Bjørke, A.K. [2010] Fast-track marine CSEM processing and 3D inversion. *72nd EAGE Conference & Exhibition*, Extended Abstracts, C004.

Received 12 September 2012; accepted 17 November 2012.

doi: 10.3997/1365-2397.2013001